International Journal of Fluid Machinery and Systems DOI: 10.5293/IJFMS.2015.8.4.318
Vol. 8, No. 4, October-December 2015 ISSN (Online): 1882-9554

Original Paper

Modeling and testing for hydraulic shock regarding a valve-less electro-hydraulic servo steering device for ships

Liao Jian[1,2], He Lin[1,2], Xu Rongwu[1,2]

1. Institute of Noise & Vibration, Naval University of Engineering
Jiefang Road NO.717, Wuhan, 430033, China, jl_zss@sina.com, lh_zss@163.com
2. State Key Laboratory of Ship Vibration & Noise, Naval University of Engineering
Jiefang Road NO.717, Wuhan, 430033, China, rw_zss@163.com

Abstract

A valve-less electro-hydraulic servo steering device (short: VSSD) for ships was chosen as a study object，and its mathematic model of hydraulic shock was established on the basis of flow properties and force balance of each component. The influence of system structure parameters, changing rate of motor speed and external load on hydraulic shock strength was simulated by the method of numerical simulation. Experiment was designed to test the hydraulic shock mathematic model of VSSD. Experiment results verified the correctness of the model, and the model provided a correct theoretical method for the calculation and control of hydraulic shock of valve-less electro-hydraulic servo steering device.

Keywords: valve-less; steering device; hydraulic shock; changing rate; accumulator; external load

1. Introduction

Due to its high efficiency, small volume weight ratio, high reliability, the valve-less electro-hydraulic servo steering device for ships, which is called VSSD for short, is being widely used in the military and civil fields [1, 2]. Featuring none of hydraulic control valves and long pipelines, the device is mainly composed of a servo motor, a pump and a hydraulic cylinder. By adjusting the motor speed to change the flow, the speed and position of the device are controlled.

When controlling the speed and position of the device, the opening and closing of valves (for the valve controlled steering device), or the starting, stopping and reversing of pump (for the VSSD) is inevitable, this may cause the sudden change of pressure and generate the hydraulic shock. The hydraulic shock can damage the seal parts, reduce reliability and the device lifetime. To make matters worse, the hydraulic shock would stimulate the transient vibration of its structures and degrade the low noise characteristics. The hydraulic shock mechanism of the valve controlled steering device has been studied in depth at home and abroad. Kane [3] has given the qualitative description of hydraulic shock mechanism. Ghidaoui [4] has done the detailed theoretical study on its "water hammer" effect which is caused by the sudden opening and closing of the valves. Fang Zhicheng and Jiang Nengjun [5] propose the measures to reduce its hydraulic shock. The theoretical and experimental research on its control strategy of hydraulic shock has been done by Feng Yuchen [6]. Regina and Geraldo use MOC to simulate the response of a pipe system upstream from power plants in the case of valve closure [7].

Currently, the researches on the VSSD are focused on its dynamic response and integrated design of structures [8-10]. However, the hydraulic shock mechanism of VSSD has not been studied. This paper aims to establish the theoretical model of VSSD's hydraulic shock mechanism and practically to verify its correctness and accuracy.

2. Theoretical model

The hydraulic shock strength is evaluated by the changing amount and rate of pressure, the theoretical model of which can be obtained [11]. Basing on this model, the quantitative analysis of VSSD's hydraulic shock is conducted. The composing schematic of VSSD is shown in Fig.1.

Received March 25 2015; revised September 24 2015; accepted for publication Novemberer 30 2015; Review conducted by Kwang-Yong Kim, PhD.(Paper number O15019K)
Corresponding author: Xu Rongwu, Associate Professor, rw_zss@163.com

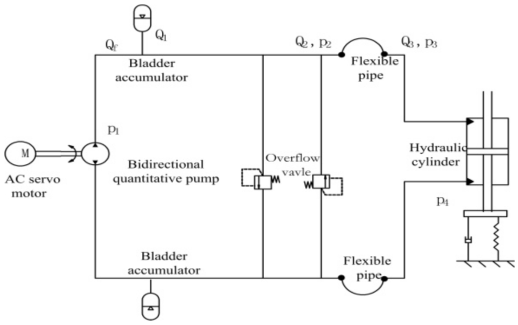

Fig.1. Composing schematic of VSSD

2.1 Flow continuity equations

The flow continuity equation inside pump is shown in eq. (1).

$$Q_f = nV_p - C_{ep} p_1 - C_{ip}(p_1 - p_4) \tag{1}$$

Where Q_f is the output flow of pump, n is the speed of AC servo motor, D is the displacement of pump, p_1 is the outlet pressure of pump, p_4 is the inlet pressure of pump, C_{ep} is the external leakage coefficient, C_{ip} is the internal leakage coefficient.

The flow continuity equation outside pump's flow is shown in eq. (2).

$$Q_f = Q_1 + Q_2 \tag{2}$$

Where Q_1 is the inlet flow of accumulator, Q_2 is the inlet flow of flexible pipe.

Paper [12] give us the impedance of the accumulator which is shown in eq. (3).

$$Z_1(s) = \frac{P_1(s)}{Q_1(s)} = \frac{2p_0}{Q_0} \frac{s^2 + 2\delta_a \omega_a s + \omega_a{}^2}{s^2 + (2\delta_a \omega_a + \frac{\omega_a{}^2}{\omega_c{}^2})s + \omega_a{}^2} \tag{3}$$

$$\omega_a = \sqrt{\frac{n' p_0 a}{\rho l_a V_a}}$$

$$\omega_c = \frac{n' Q_0}{2V_a}$$

$$\delta_a = \frac{16v}{d_a{}^2 \omega_a}$$

Where ω_a is the natural frequency of accumulator, ω_c is its cut-off frequency, δ_a is its damping ratio, a is the cross-sectional area of the connecting pipe of accumulator, n' is the air polytropic exponent, v is the oil flow rate in the connecting pipe of accumulator, d_a is the diameter of the connecting pipe of accumulator, l_a is the length of the connecting pipe of accumulator, p_0 and Q_0 denote the rated pressure and the rated flow respectively.

2.2 Pipe dynamic equations

The function of the flexible pipe in this paper is to channel the high pressure oil from the hydraulic pump to the hydraulic cylinder. There are mainly three methods of modeling the dynamic behavior of the fluid within the pipe: the simplified modeling method, the lumped parameter modeling method and the distribution parameter modeling method [13].

The simplified modeling method is to describe the pipe as a concentrated capacity. No the length, resistance of the pipe and material properties of the fluid are considered. The pipe has no dynamics. Such a model only provides the approximate results.

The lumped parameter modeling method is to regard the pipe as the lumped resistance, the lumped capacity and the lumped inductance which are connected in series. Pressure and flow variation is only monitored at the beginning and at the end of the pipe. Dynamics of the fluid within the pipe is not considered. The model based on this method is only suitable for the calculation of dynamics of the low frequency pulsation fluid within the short pipe. The big calculation error would generate when the pulsation frequency is high or the pipe length is long.

The model built by the distribution parameter modeling method is based on the Law of conservation of mass, Navier-Stokes Law and fluid properties. Such a model has an advantage in high precision of calculation, which is applicable to the calculation of dynamics of the fluid with the wide range frequency of pulsation within the long pipe.

As the hydraulic shock has the wide range frequency of pulsation and the hose pipe length is comparatively long, the dynamics equation of the hose pipe is obtained by the distribution parameter modeling method [14].

$$\begin{bmatrix} p_2(s) \\ Q_2(s) \end{bmatrix} = \begin{bmatrix} A_{11} & A_{12} \\ A_{21} & A_{22} \end{bmatrix} \begin{bmatrix} p_3(s) \\ Q_3(s) \end{bmatrix}$$
$$A_{11} = A_{22} = ch\Gamma(s)l$$
$$A_{12} = Z_0(s)sh\Gamma(s)l \tag{4}$$
$$A_{21} = \frac{1}{Z_0(s)} sh\Gamma(s)l$$
$$Z_0(s) = \frac{\rho c^2 \Gamma(s)}{\pi r_0{}^2 s}$$
$$\Gamma(s) = \frac{s}{c}\left\{1 - \frac{2}{ir_0(\frac{s}{\upsilon})^{1/2}} \frac{J_1(ir_0(\frac{s}{\upsilon})^{1/2})}{J_0(ir_0(\frac{s}{\upsilon})^{1/2})}\right\}^{-1/2}$$

Where $Z_0(s)$ is the characteristic impedance of flexible pipe, $\Gamma(s)$ is its transmission coefficient, c is the sound speed in the flexible pipe, r_0 is the radius of flexible pipe, υ is the kinetic viscosity of hydraulic oil, J_1 is the first-order Bessel function, J_0 is the zero-order Bessel function, s is the Laplace operator.

2.3 Flow continuity and equilibrium equations of hydraulic cylinder

The flow continuity equation of hydraulic cylinder is shown in eq. (5).

$$Q_3 = A\frac{dx}{dt} + \frac{V_c}{\beta}\frac{dp_3}{dt} + C_{tm}p_3 \tag{5}$$

Where A is the effective area of hydraulic cylinder, V is the volume of its controlled chamber, β is the effective bulk modulus of hydraulic oil, C_{tm} is its total leakage coefficient.

The equilibrium equation of hydraulic pressure can be obtained.

$$(p_3 - p_4)A = m\frac{d^2x}{dt^2} + B_v\frac{dx}{dt} + kx + F_f + F_L$$
$$F_f = \begin{cases} F_c sign(\dot{x}), \dot{x} \neq 0 \\ F_s, \dot{x} = 0 \end{cases} \tag{6}$$
$$sign(\dot{x}) = \begin{cases} +1, \dot{x} > 0 \\ -1, \dot{x} > 0 \end{cases}$$

Where m is the total mass of piston rod and load object, B_v is its velocity viscous coefficient, F_c is the coulomb friction, F_s is the static friction, k is the elastic load stiffness, F_L is the external load force.

2.4 Theoretical model of hydraulic shock

As p_4 is far less than p_1, p_4 is replaced with zero. Use the changing amount and rate of inlet pressure p_3 of hydraulic cylinder to quantify hydraulic shock strength. After conducting Laplace transform on eq. (1), (5) and (6) ,and then combine them with eq. (2) and (4), the theoretical frequency domain model of hydraulic shock can be deduced.

$$p_3(s) = \frac{nV_p + \dfrac{A_{12}}{\dfrac{1}{Z_1(s)} + C_{tp}} F_L A}{A_{21} + \dfrac{A_{22}}{Z_2(s)} + (\dfrac{1}{Z_1(s)} + C_{tp})(A_{11} + \dfrac{A_{12}}{Z_2})}$$
$$Z_2(s) = \frac{1/A^2}{\dfrac{s^2}{\omega_h{}^2} + \dfrac{2\xi_h}{\omega_h}s + 1}$$
$$\omega_h = \sqrt{\frac{A^2\beta}{mV_c}} \tag{7}$$
$$\xi_h = \frac{(V_c B_v/\beta + m(C_{tp} + C_{tm})}{2A^2}\omega_h$$

Where $Z_2(s)$ is the inlet characteristic impedance of hydraulic cylinder, ω_h is the VSSD's natural frequency, $C_{tp} = C_{ep} + C_{ip}$ is the total leakage coefficient of pump， ξ_h is the damping ratio [15].

According to eq. (7), the theoretical model of VSSD's hydraulic shock is a complex nonlinear model which is influenced by many parameters. The VSSD's hydraulic shock is caused by the sudden change of AC servo motor speed and external load， the strength of which is jointly determined by its structural parameters, changing rate of motor speed and external load.

3. Numerical simulation

Based on the theoretical frequency domain model, write calculation program in Matlab/Simulink. Then, the influence of the structural parameters, changing rate of motor speed and external load on hydraulic shock strength is analyzed in both time domain and frequency domain by using the parameter values shown in table 1.

Table 1 Major parameter value

Parameters	Unit	Value
ρ	kg/m^3	860
β	Pa	6×10^8
A	m^2	0.0672
V	m^3	0.043
C_{tm}	m^3/s/Pa	4.97×10^{-10}
C_{tp}	m^3/s/Pa	9.13×10^{-10}
V_p	mL/rev	63
r_0	m	0.016
E	Pa	5×10^8
M	kg	250
B_v	N/m/s	150
p_0	Pa	10×10^6
Q_0	m^3/s	1.6×10^{-3}

3.1 Influence of the structural parameters

The main structural parameters influencing hydraulic shock strength contains the pump displacement, the inlet impedance of accumulators and the structural parameters of flexible pipes, etc. In this section, it is analyzed that the influence of inlet impedance of accumulators on the inlet pressure of hydraulic cylinder p_3 under the hydraulic shock condition. The results are shown in Fig. 2, Fig. 3 and table 2.

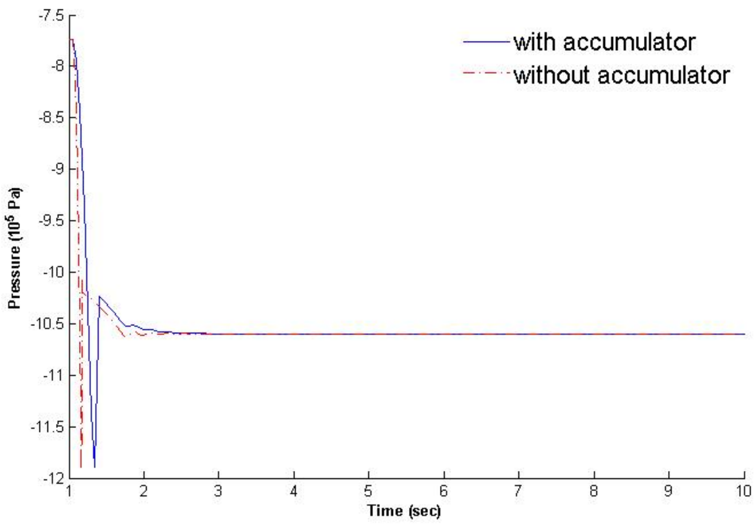

Fig.2 Time domain graph of influence of accumulator

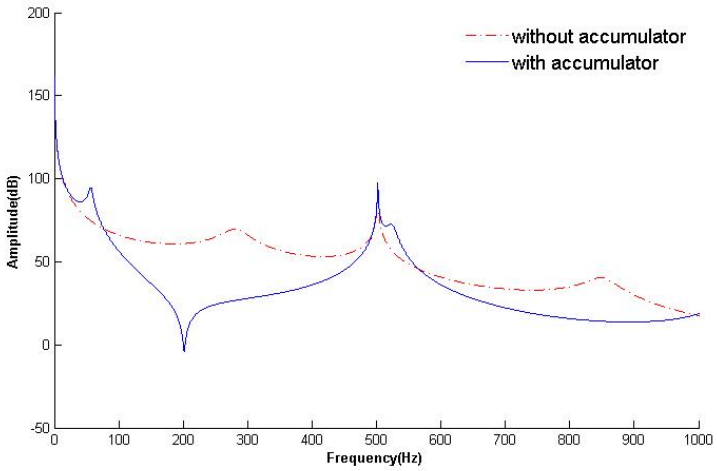

Fig.3 Frequency domain graph of influence of accumulator

Fig.2 and table 2 shows that the accumulator can decrease changing rate of pressure, which can reduce the hydraulic shock strength. Furthermore, Fig.3 shows that accumulator can reduce the effect in a certain frequency band, especially near the natural frequency (200 Hz), which obtains attenuation effect 63dB. So the hydraulic shock can be reduced in the hardware configuration.

It is important to note that the peak amplitude generates at 502.3 Hz whether is with accumulator or without accumulator. The reason for this is that the VSSD's natural frequency ω_h equals to 502.3Hz, which cause the resonance phenomenon at this frequency point.

Table 2 Comparison of pressure rise and changing rate

	Changing amount of pressure Pa	Changing rates of pressure Pa /s
Without accumulator	-4.17×10^5	-30.89×10^5
With accumulator	-4.16×10^5	-11.21×10^5

3.2 Influence of the changing rate of motor speed

When the motor speed changes, the flow changes which would causes the pressure change and generate hydraulic shock. The changing rate of motor speed is the software configuration parameter as it can be adjusted by changing the control parameters. Influence of the different changing rates of motor speed on the inlet pressure p_3 of hydraulic cylinder is analyzed in this section. The results are shown in Fig.4 and Fig.5.

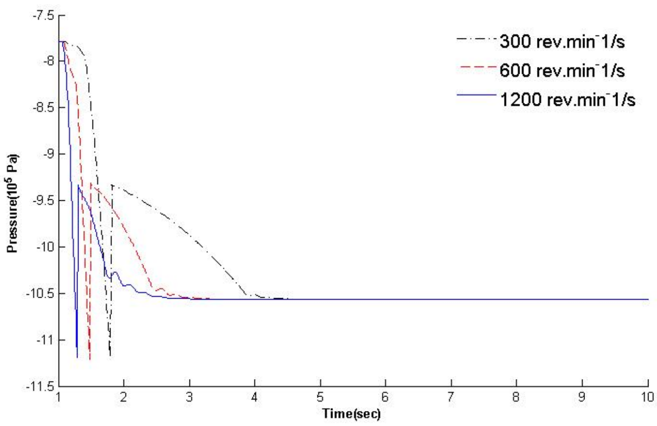

Fig.4 Time domain graph of influence of changing rate of motor speed

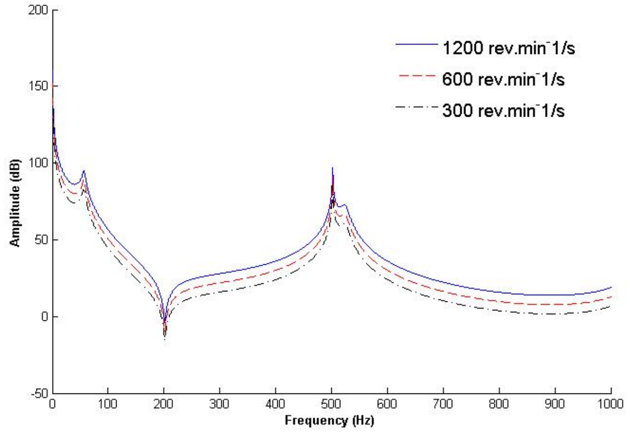

Fig.5 Frequency domain graph of influence of changing rate of motor speed

Fig.4 shows that the smaller the changing rate of motor speed is, the lower the hydraulic shock strength is. Fig.5 shows that decreasing the changing rate of motor speed can reduce the hydraulic shock in a wide broadband. For the VSSD in this paper, when the changing rate of motor speed drop by half, the amplitude of pressure variation by the hydraulic shock in frequency domain decreased by 6.02 dB.

3.3 Influence of the changing rate of external load

The variation of external load can cause the change of pressure in the VSSD, which arouse the hydraulic shock. The changing rate of external load is perturbed parameter as it has some uncertainty. The influence on the inlet pressure p_3 of hydraulic cylinder caused by step variable load and slope variable load is analyzed in this section. The results are shown in Fig.6 and Fig.7.

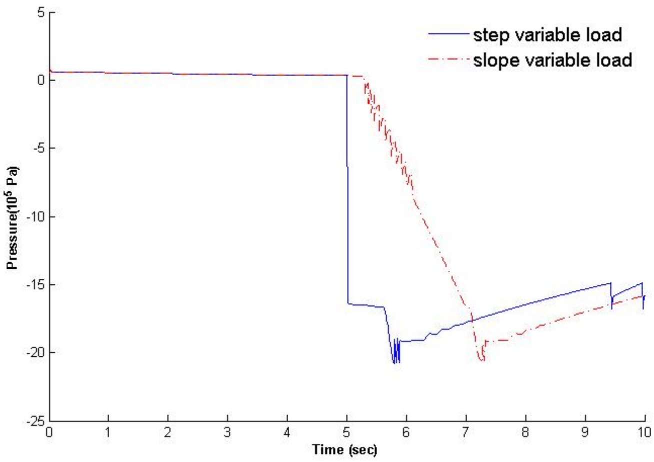

Fig.6 Time domain graph of influence of the changing rate of external load

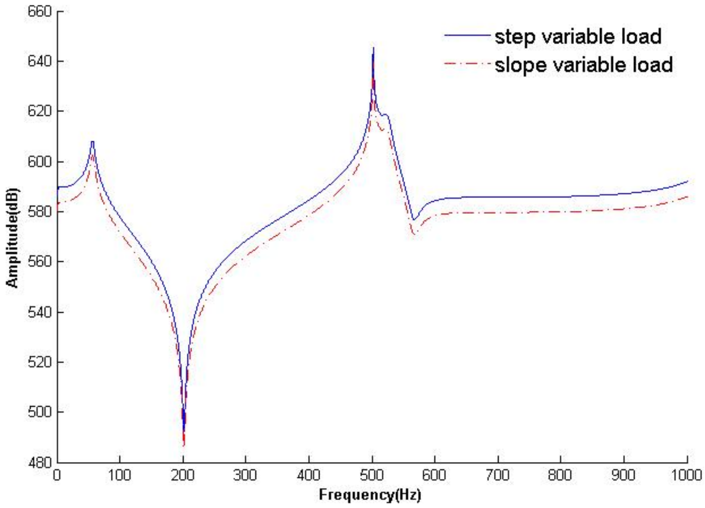

Fig.7 Frequency domain graph of influence of the changing rate of external load

Fig.6 shows that the changing rate of pressure caused by step variable load is greater than that caused by slope variable load. Furthermore, Fig.7 shows that the amplitude of pressure variation caused by step variable load is higher on the average 6dB than that caused by slope variable load in frequency domain.

4. Experimental verification

4.1 Experimental scheme

In order to verify the correction and accuracy of the theoretical model of hydraulic shock in the VSSD, the experiment is conducted in the device shown in Fig.8.

Fig.8 The valve-less electro-hydraulic servo steering device prototype

The basic experimental steps is that hydraulic shock under different changing rate of motor speed is simulated by changing the motor speed rate, and the data of pressure is recorded by pressure transducers on the VSSD.

4.2 Experimental results

The data is processed and compared with the simulation results. The comparison results are shown in Fig.9, Fig.10, table 3 and table 4.

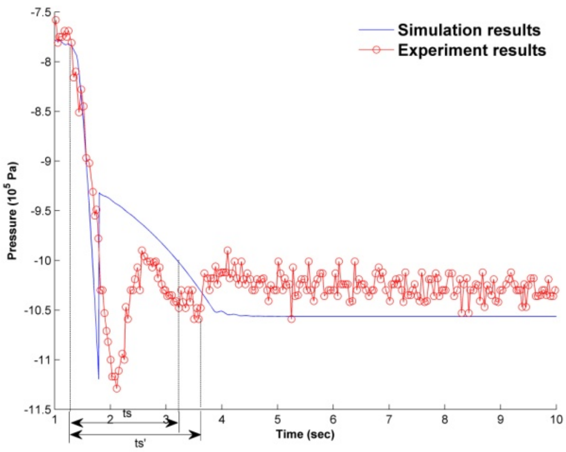

Fig.9 Comparison between simulation and experiment at 1200 rev.min^{-1}/s

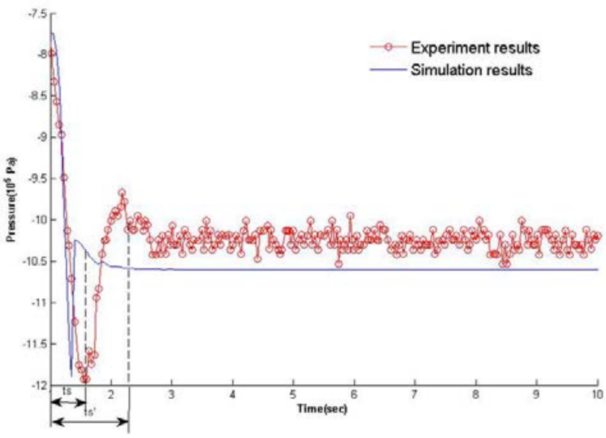

Fig.10 Comparison between simulation and experiment at 300 rev.min^{-1}/s

Fig.9 and Fig.10 show that the changing tendency of the simulation results correspond with that of experimental results. However, table 3 and table 4 shows that errors of hydraulic shock strength between experimental results and simulation results exist.

Table 3 Comparison at 1200 rev.min^{-1}/s

	Simulation result	Experimental result	error

Changing amount of pressure Pa	-4.156×10^5	-4.182×10^5	0.6%
Changing rate of pressure Pa/s	-7.556×10^5	-6.508×10^5	16.1%

Table 4 Comparison at 300 rev.min^{-1}/s

	Simulation result	Experimental result	error
Changing amount of pressure Pa	-3.390×105	-3.540×10^5	4.2%
Changing rate of pressure Pa/s	-5.060×10^5	-4.097×10^5	23.5%

4.3 Errors analysis

The errors mainly derive from the following three aspects:

(1) In the experiments, the actual changing rate of motor speed is less than the setting changing rate of motor speed, which causes that the results of changing pressure rate from experiments is less than those from simulation.

(2) The characteristics of load simulator are not considered in the theoretical model of hydraulic shock. For example, the inertia of the load simulator increases the VSSD's inertia load, which causes that the results of adjustment time of hydraulic pressure oscillation from experiments is larger than those from simulation.

(3) Constants in theoretical calculation are not fixed, which would vary with the condition. For example, the elasticity modulus of oil is various with the air content in oil.

5. Conclusion

The theoretical model of VSSD is deduced by the flow continuity equation, pipe dynamic equations, flow continuity and equilibrium equation of hydraulic cylinder. Basing on this model, the influence on hydraulic shock strength caused by structural parameters, changing rate of motor speed and external load is analyzed. Experimental results verify the correctness and accuracy of the theoretical model, which is of significance and practical value to the calculation and control of hydraulic shock.

Acknowledgement

This work is supported by the National Science Key Lab Fund project(NO.SYSZC2014004,China) and the Navy Pre-research project. These supports are gratefully acknowledged.

Nomenclature

A	the effective area of hydraulic cylinder [m^2]
a	the cross-sectional area of the connecting pipe of accumulator [m^2]
B_v	the velocity viscous coefficient [N/m/s]
C_{ep}	the external leakage coefficient [m^3/s/Pa]
C_{ip}	the internal leakage coefficient [m^3/s/Pa]
C_{tm}	the total leakage coefficient of hydraulic cylinder [m^3/s/Pa]
C_{tp}	the total leakage coefficient of pump [m^3/s/Pa]
c	the sound speed in the flexible pipe [m/s]
d_a	the diameter of the connecting pipe of accumulator [m]
E	the Young's modulus of flexible pipe [bar]
Q_f	the output flow of pump [m^3/s]
n	the speed of AC servo motor [rev/min]
F_c	the Coulomb friction [N]
F_s	the static friction [N]
F_L	the external load force [N]
J_1	the first-order Bessel function
J_0	the zero-order Bessel function
k	the elastic load stiffness [N/m]
l_a	the length of the connecting pipe of accumulator [m]
m	the total mass of piston rod and load object [kg]
n'	the air polytropic exponent
p_0	the rated pressure [Pa]
p_1	the outlet pressure of pump [Pa]
p_4	the inlet pressure of pump [Pa]
Q_0	the rated flow [m^3/s]
Q_1	the inlet flow of accumulator [m^3/s]
Q_2	the inlet flow of flexible pipe [m^3/s]
r_0	the radius of flexible pipe [m]
V_p	the displacement of pump [m^3/rev]
V	the volume of its controlled chamber [m^3]
v	the oil flow rate in the connecting pipe of accumulator [m/s]
$Z_0(s)$	the characteristic impedance of flexible pipe
$Z_2(s)$	the inlet characteristic impedance of hydraulic cylinder
ω_a	the natural frequency of accumulator [Hz]
ω_c	the cut-off frequency [Hz]
δ_a	the damping ratio
$\Gamma(s)$	the transmission coefficient
ω_h	the natural frequency [Hz]
ξ_h	the damping ratio
β	the effective bulk modulus of hydraulic oil [Pa]
υ	the kinetic viscosity of hydraulic oil [m^2/s]

Reference

[1] Nakano, K. and Tanaka, Y., 1988, “Energy Saving Type Electro Hydraulic Servo System,” Journal of Fluid Control, Vol.18, No.3, pp.35-51.

[2] Office of Naval Research, 2008, “Electrically Actuated Submarine Control Surfaces,” http://www.onr.navy.mil/02/ccr.htm.

[3] Kane, J. and Richmond, T. D., 1965, “Noise in Hydrostatic Systems and its Suppression,” Proceedings of the Institution of Mechanical Engineers, UK,GT-1965-18036.

[4] Ghidaoui, M.S. and Mansour, S., 2002, “Efficient Treatment of the Vardy-Brown Unsteady Shear in Pipe Transients,” Hydraulic Engineering, Vol.128, No.1, pp.102–112.

[5] Fang, Z. C. and Jiang, N.J., 2004, “Investigation on Hydraulic Shock of Submarine Steering System,” Ship & Ocean Engineering, No.3, pp.31-33.

[6] Feng, Y. Liu, Q. and Wu, X.Y., 2009, “Application of the Dynamically Compensation Method in the Control of the Steering Electro-hydraulic Actuator System,” Ship & Ocean Engineering, Vol.38, No.1, pp.29-31.

[7] Regina, M. B, Geraldo, L. T. Ivan, F. S., 2015, “Case studies for solving the Saint-Venant equations using the method of characteristics: pipeline hydraulic transients and discharge propagation,” International Journal of Fluid Machinery and Systems, Vol.8, No.1, pp.55-62.

[8] Wang, W., 2008, “Research on Performance and Refit Design of Direct Volume Control Electro-Hydraulic Servo Cylinder,” Master of Engineering, Harbin Institute of Technology, Harbin.

[9] Navarro, R., 1997, “Performance of an Electro-Hydrostatic Actuator on the F-18 Systems Research Aircraft,” NASA/TM-97-206224.

[10] Williams, K. and Brown, D., 1997, “Electrically Powered Actuator Design,” NASA/USAF/Navy.

[11] Fu, Y. L. Zhao, K. and Qi, X.Y., 2010, “Modeling and Reducing of Water Hammer of Proportion Direction Valve Controlled Ship Steering System,” Journal of Beijing University of Aeronautics and Astronautics, Vol.36, No.6, pp.640-644.

[12] Ren, Z.G.,2006, “Modeling and Simulation of Hydraulic Noise of Steering System of Certain Ship, “Master of Engineering, Huazhong University of Science&Technology, Wuhan.

[13] Lovrec, D. Kastrevc, M, 2011, “Modelling and Simulating a Controlled Press-Brake Supply System,” Int J Simul Model, Vol.10, No.3, pp: 133-144.

[14] Johnston, D.N., 2002, “The Transmission Line Method for Modeling Laminar Flow of Liquid in Pipelines,” http://dx.doi.org/10.1177/0959651811430035.

[15] Yi, M.L. Cao, S.P and Liu, Y.S., 2013, Electro-Hydraulic Servo Control Technology, Press of Huazhong University of Science&Technology ,Wuhan.